GA–A25804

ELECTRON CYCLOTRON CURRENT DRIVE AT HIGH ELECTRON TEMPERATURE ON DIII–D

by
C.C. PETTY, M.E. AUSTIN, R.W. HARVEY, J. LOHR,
T.C. LUCE, M.A. MAKOWSKI, and R. PRATER

MAY 2007

GENERAL ATOMICS

DISCLAIMER

GA–A25804

ELECTRON CYCLOTRON CURRENT DRIVE AT HIGH ELECTRON TEMPERATURE ON DIII–D

by
C.C. PETTY, M.E. AUSTIN,* R.W. HARVEY,† J. LOHR,
T.C. LUCE, M.A. MAKOWSKI,‡ and R. PRATER

This is a preprint of a paper to be presented at the 17th Topical Conference on Radio Frequency Power in Plasmas, Clearwater, Florida, May 7–9, 2007, and to be published in the *Proceedings.*

*University of Texas at Austin, Austin, Texas
†CompX, Del Mar, California
‡Lawrence Livermore National Laboratory, Livermore, California

Work supported by
the U.S. Department of Energy
under DE-FC02-04ER54698, DE-FG03-97ER54415,
DE-FG03-99ER54541, and W-7405-ENG-48

GENERAL ATOMICS PROJECT 30200
MAY 2007

GENERAL ATOMICS

ABSTRACT

Experiments on DIII-D have measured the electron cyclotron current drive (ECCD) efficiency for co- and counter-injection in low density plasmas with radiation temperatures from electron cyclotron emission (ECE) above 20 keV. The radiation temperature is generally higher than the Thomson scattering temperature, indicating that there is a significant population of non-thermal electrons. The experimental ECCD profile measured with motional Stark effect (MSE) polarimetry is found to agree with quasi-linear theory except for the highest power density cases (Q_{EC}/n_e^2»1). Radial transport of the energetic electrons with diffusion coefficients of ~0.4 m^2/s is needed to model the broadened ECCD profile at high power density.

I. INTRODUCTION

There are several important applications on ITER for the localized non-inductive current generated by electron cyclotron waves, including suppression of neoclassical tearing modes (NTM) [1,2]. While electron cyclotron current drive (ECCD) has been extensively studied and compared to linear and quasi-linear models [3], most experimental tests have been at electron temperatures (T_e) an order of magnitude lower than expected on ITER. Thus, there remains a need to validate ECCD theory in the ITER temperature regime. On DIII-D, experiments have measured the ECCD efficiency for co- and counter-injection in low density plasmas with radiation temperatures from electron cyclotron emission (ECE) above 20 keV. In addition, these experiments have investigated the effect of radial transport of the current carrying electrons in high T_e, high power density discharges. This is of interest because both the radial profile and total magnitude of ECCD are important to its applications.

II. HIGH ELECTRON TEMPERATURE REGIME

Nearly central ECCD is studied in low density L-mode plasmas on DIII-D during the sawtooth-free period, as seen in Fig. 1. The 110 GHz waves are launched with X-mode polarization and are absorbed at the second harmonic electron cyclotron resonance. The wave parallel index of refraction is $N_{||} = \pm 0.23$ for co/counter injection. Magnetohydrodynamic (MHD)-quiescent discharges are needed since the driven current profile is determined from the motional Stark effect (MSE) signals using the poloidal flux diffusion equation [4]. Neutral beam injection (NBI) during the current plasma rampup raises T_e and slows the resistive evolution of the current profile, delaying the onset of sawteeth. The ECCD is measured during an interval of ≥ 0.4 s soon after the current flat top is reached. During this phase, NBI is reduced to the bare minimum for MSE acquisition to minimize the injection of cold electrons, allowing the highest possible T_e to be achieved.

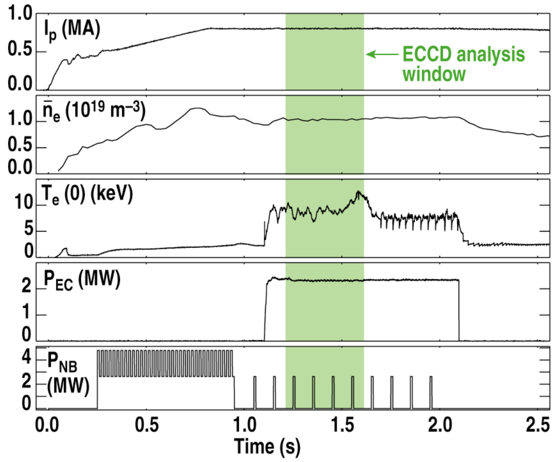

Fig 1. Time history of ECCD discharge 117940 showing use of NBI for preheating and collection of MSE data.

A narrow ECCD profile is measured for the lowest power density cases, as seen in Fig. 2. The current density driven by a single gyrotron (injected power $P_{EC} = 0.58$ MW) at modest electron density ($n_e = 3.2 \times 10^{19}$ m^{-3}) is determined by subtracting the non-inductive current profile for radial-injection from that for co-injection [4]. Figure 2 shows that the experimental ECCD profile is in agreement with the quasi-linear CQL3D Fokker-Planck code [5] assuming no radial transport of the electrons. In Fig. 3, the total ECCD measured in the same manner is compared with the CQL3D code for plasmas with T_e from Thomson scattering between 5.8–11.3 keV, n_e between 1.2 – 3.2 × 10^{19} m^{-3}, and P_{EC} between 0.55–2.3 MW. This data set extends DIII-D measurements of ECCD to ~70% higher thermal T_e than previously studied. Good agreement is found for the low power density cases ($Q_{EC}/n_e^2 < 0.7$, where Q_{EC} is the rf power density in MW/m^3 and n_e is in units of 10^{19} m^{-3}), but for the high power density cases ($Q_{EC}/n_e^2 > 2.6$) the experimental ECCD falls short. Note that for $Q_{EC}/n_e^2 > 0.5$ the ECCD efficiency is expected to be power dependent [6], and the ECCD quasi-linear enhancement is ~30% for these plasmas.

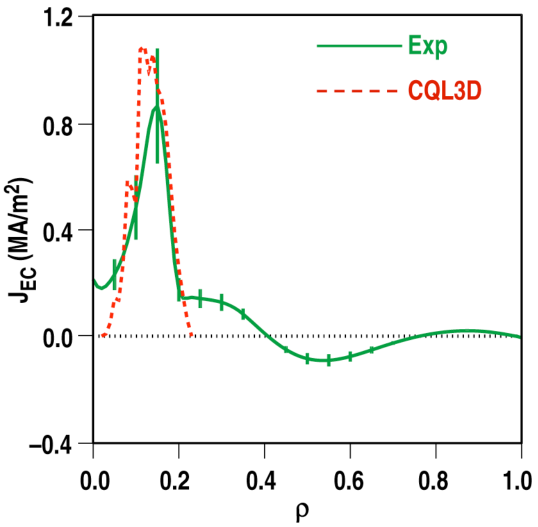

Fig 2. Radial profiles of experimental ECCD and CQL3D modeling for $Q_{EC}/n_e^2 = 0.16$.

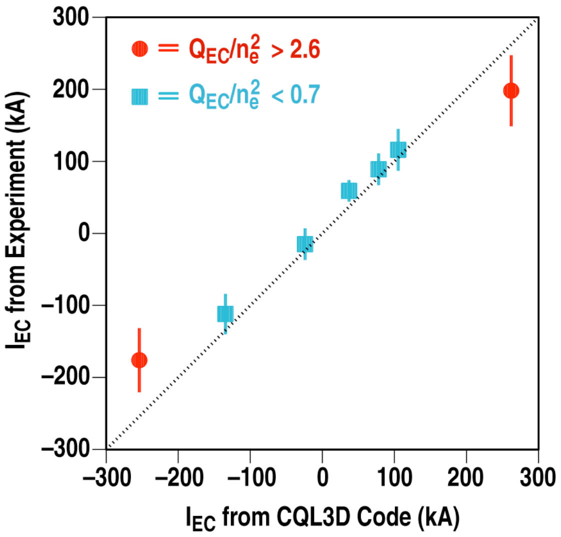

Fig 3. Comparison of experimental and theoretical ECCD magnitude.

An anomalously high radiation temperature indicates that the high power density cases have a significant population of non-thermal electrons that is largest for counter-injection, less for co-injection, and smallest for radial injection. Figure 4 plots the T_e profiles measured by ECE and Thomson scattering for plasmas with $Q_{EC}/n_e^2 > 2.6$. While fair agreement between these diagnostics is found for radial-injection, the central radiation temperature is ≈ 2 times higher than Thomson scattering for co-injection and ≈ 3 times higher for counter-injection (exceeding 20 keV). The high T_e edge points from ECE reflect non-thermal emission at the third harmonic on the high field side of the plasma. The CQL3D code predicts significant non-thermal effects for these high power density cases, most notably flattening of the electron distribution function at low velocities for co/counter injection. (Note that the nonthermal effects on the bulk are not yet fully accounted for in CQL3D.) The radiation temperature calculated using the CQL3D electron distribution function for counter-ECCD is four times higher than the actual temperature, similar to Fig. 4, and the modeled ECE profile reproduces the observed high-field-side/low-field-side asymmetry as well.

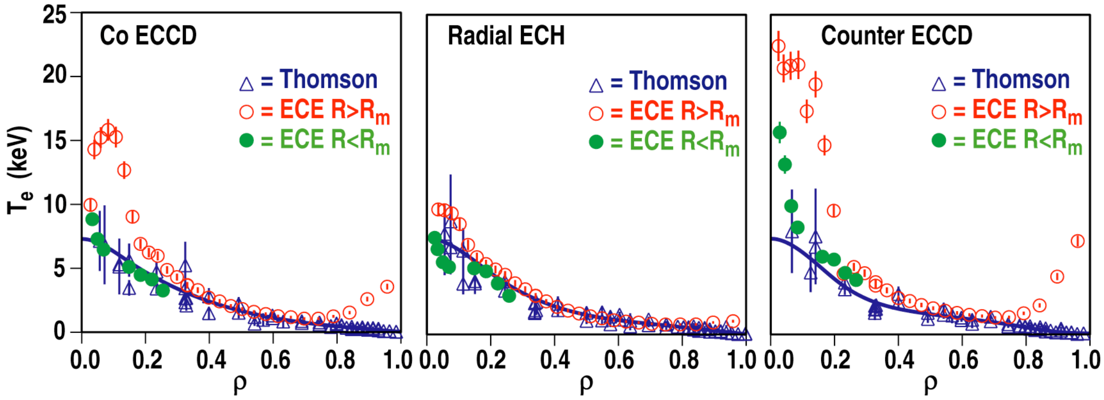

Fig 4. Electron temperature profiles measured by ECE and Thomson scattering for $Q_{EC}/n_e^2 > 2.6$.

III. EFFECT OF ELECTRON TRANSPORT

Radial transport of current carrying electrons may explain the lower ECCD for the high power density cases. Figure 5 shows that the experimental ECCD profile for the $Q_{EC}/n_e^2 = 2.6$ case is clearly broader than the CQL3D prediction assuming no radial transport. Including an *ad hoc* electron diffusion coefficient (central value D_{rr0}) in CQL3D reduces and broadens the ECCD profile, bringing theory and experiment into better agreement. At high power density, the total driven current from CQL3D agrees with the measured value (to within the measurement uncertainties) for D_{rr0} between 0.1–1 $\mathrm{m^2/s}$. A tighter constraint can be placed on D_{rr0} by comparing the measured and modeled current densities. Figure 5 shows that $D_{rr0} = 0.4\ \mathrm{m^2/s}$ reproduces well the measured ECCD profile, but $D_{rr0} = 1\ \mathrm{m^2/s}$ produces too broad of a profile. This result is consistent with previous work on DIII-D that determined D_{rr0} must be $\leq 0.7\ \mathrm{m^2/s}$ to be consistent with direct ECCD measurements and NTM stabilization experiments [2,7]. This best fit value of D_{rr0} is an order of magnitude less than the electron thermal diffusivity, but it is comparable to the effective particle diffusion coefficient.

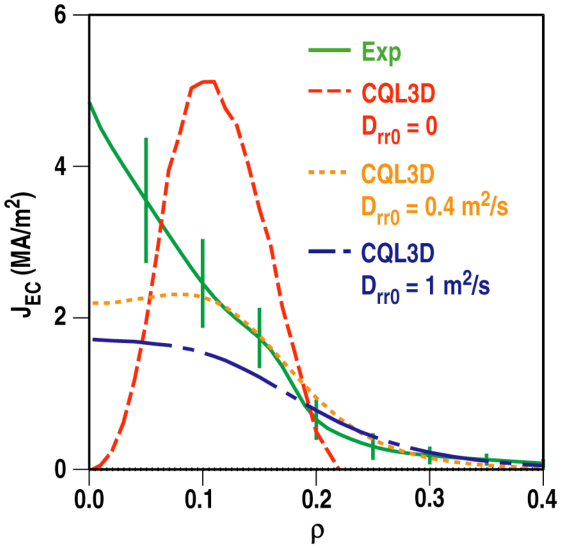

Fig 5. Radial profiles of experimental ECCD and CQL3D modeling for $Q_{EC}/n_e^2 = 2.6$.

The effect of radial transport is weaker in low power density cases, but small amounts of electron diffusion can still be present. Compared to Fig. 5, higher density cases with $Q_{EC}/n_e^2 = 0.34$ have a more localized experimental ECCD profile that is best modeled by CQL3D using $D_{rr0} = 0.1$–$0.2\ \mathrm{m^2/s}$. The case with $Q_{EC}/n_e^2 = 0.16$ shown in Fig. 2 is consistent with $D_{rr0} = 0$. Thus, the electron diffusion coefficient may be power density (or more simply, electron density) dependent. It is worth mentioning that the total driven current calculated by CQL3D decreases with increasing D_{rr0} three times more slowly for high density plasmas than for low density plasmas. This is because the shorter electron slowing down time gives radial transport less time to have an effect.

IV. SUMMARY

Experiments on DIII-D have measured up to 200 kA of ECCD in low density L-mode plasmas with thermal $T_e \sim$ 10 keV. The radiation temperature from ECE can exceed 20 keV, indicating that the non-thermal electron population is significant. The ECCD profile determined by MSE polarimetry agrees with the CQL3D code except when Q_{EC}/n_e^2»1. However, the reduced and broadened ECCD profile at these high power densities can be reproduced in CQL3D by including an electron diffusion coefficient of ~ 0.4 m^2/s. Fortunately, this level of radial transport will have only a modest effect on the application of ECCD in high density H-mode plasmas.

REFERENCES

[1] C. C. Petty *et al.*, *Nucl. Fusion* **44** (2004) 243-251.

[2] C. C. Petty *et al.*, “Complete Suppression of the m=2/n=1 NTM Using ECCD on DIII-D,” in *15th Int. Conf. on Radio Frequency Power in Plasmas-2003*, edited by C. B. Forest, AIP Conference Proceedings 694, American Institute of Physics, Melville, NY, 2003, pp. 348-351.

[3] R. Prater, *Phys. Plasmas* **11** (2004) 2349-2376.

[4] C. B. Forest *et al.*, *Phys. Rev. Lett.* **73** (1994) 2444-2447.

[5] R. W. Harvey and M. G. McCoy, “The CQL3D Fokker-Planck Code,” in *Proc. IAEA Technical Committee Meeting-1992*, International Atomic Energy Agency, Vienna, 1993, pp. 498.

[6] R. W. Harvey, M. G. McCoy, and G. D. Kerbel, *Phys. Rev. Lett.* **62** (1989) 426-429.

[7] C. C. Petty *et al.*, *Nucl. Fusion* **43** (2003) 700-707.

ACKNOWLEDGMENT

This work supported by the U.S. Department of Energy under DE-FC02-04ER54698, DE-FG03-97ER54415, DE-FG03-99ER54541, and W-7405-ENG-48.